STATIC FORMATION CONTROL USING INTERSPACECRAFT COULOMB FORCES

Gordon G. Parker, Chris E. Passerello, and Hanspeter Schaub

2nd International Symposium on Formation Flying Missions and Technologies

Washington, D.C. Sept. 14–16,2004

Static Formation Control Using Interspacecraft Coulomb Forces

Gordon G. Parker * and Chris E. Passerello †

Michigan Technological University, Houghton, MI, 49931, USA

Hanspeter Schaub ‡

Virginia Poytechnic and State University, Blacksburg, VA, 24061, USA

A pair of charged bodies exerts equal and opposite Coulomb forces on each other that are proportional to the square of their charge and inversely proportional to the square of their separation distance. Exploiting these forces, for the purpose of spacecraft formation flying, has been the focus of several recent studies. This paper presents a sequential control strategy for arranging N charged bodies into an arbitrary geometry using $N+3$ participating bodies. The approach overcomes two challenging aspects of Coulomb force control: (1) the Coulomb force coupling, and (2) inadmissable control solutions arising from the square force nonlinearity. A simulation example is included that illustrates the three-dimensional repositioning of a single charge body. All bodies are assumed to be on inter-planetary trajectories where the orbital mechanics can be neglected and the Coulomb attraction is the dominant force.

I. Introduction

The practicality of developing useful Coulomb force levels for formation flying applications was originally considered by King et al.[1] Based on data gathered during the SCATHA[2] and ATS[3] missions it was concluded that interspacecraft Coulomb forces from 10 to 100 micro Newtons could be generated for high Earth orbit (HEO) formation flying missions. Low Earth orbit (LEO) applications were considered unlikely due to the small LEO Debye length (< 10cm), λ_d. More specifically, the interspacecraft Coulomb force F_c between two bodies, denoted 1 and 2, is

$$F_c = k_c \frac{q_1 q_2}{d_{12}^2} e^{-d_{12}/\lambda_d} \tag{1}$$

where k_c is Coulomb's constant ($8.99 \cdot 10^9 Nm^2/C^2$), q_i the charge on the i-th spacecraft's charge device, and d_{12} is the distance between charged bodies. Since HEO Debye lengths are estimated to range from 140 meters to 1400 meters, Coulomb force formations with spacecraft distances of 10 meters to 100 meters are possible. For example, consider a formation in HEO where the charging elements are spherical. The relationship between charge and voltage is

$$V_i = \frac{q_i k_c}{r_{i,s/c}} \tag{2}$$

where $r_{i,s/c}$ is the radius of the i-th spacecraft. For $r_{i,s/c}$ of 0.5 meters, d_{12} of 10 meters and $V_i = 10,000$ volts, the interspacecraft Coulomb force is approximately 28 micro Netwons, which is comparable to existing electric propulsion technologies.

Based on the observation that useable Coulomb forces were readily attainable and that this form of propulsion was nearly propellantless, the ability to generate static formations was considered.[4] The creation of crystal-like formations was demonstrated with the spacecraft maintaining non Keplarian orbits. Although

*Associate Professor, Mechanical Engineering - Engineering Mechanics Dept., Houghton, MI 49931.

†Professor, Mechanical Engineering - Engineering Mechanics Dept., Houghton, MI 49931.

‡Assistant Professor, Aerospace and Ocean Engineering Dept., Blacksburg, VA, 24061.

equilibrium configurations existed, none were found to be stable, resulting in the need for closed loop control. The most promising Coulomb force control strategy thus far is a bounded orbit element error approach, developed for 2 spacecraft.[5]

The main conclusions from the previous work in this field is that interspacecraft Coulomb forces are viable for both formation shape and attitude maintenance. However, even if the formation center of mass is static (i.e. formation is far removed from attracting body), the control problem is formidable due to the highly coupled nonlinear behavior of the system dynamics. In addition, the square nonlinearity in the input force, such as the $q_1 q_2$ term in Eq. 1 introduces difficulties in generating the control law when considering three or more bodies as described by Schaub et al.[5] This paper presents a control strategy that addresses these problems for non orbiting charged bodies. Clearly this is an easier problem then the more general case of an orbiting formation. However, it is expected that control approaches developed for simple charged bodies will provide insight on how to solve the similar problem that includes orbital dynamics. A typical mission scenario is as follows. Consider a set of sensors that need to be placed very accurately relative to each other. Maneuvering the sensor vehicles is a challenging problem, even without orbital mechanics, due to the control bandwidth limitations of common thrusting technologies. The proposed concept discussed here will use three *drone* spacecraft whose sole purpose is to move the sensor spacecraft. Exploiting Coulomb propulsion, this is accomplished without physical contact and using essentially no fuel on the sensor craft. These craft will be charged to a known level one at a time. The drone craft will then charge themselves to push and pull the sensor craft into the required position using electric fields. Due to the very high bandwidth of the Coulomb control, this can be accomplished very accurately. Furthermore, after the maneuver is complete the sensor vehicle is completely decoupled from the drones simply be setting the sensor vehicle charge to zero.

The remainder of the article is organized as follows. Section II describes the sequential control approach with a simulation example in Section III. Conclusions and some ideas for future work are provided in Section IV.

II. Sequential Coulomb Shape Control

Consider N charged bodies with masses m_i at rest in the absence of any external field, as shown in Figure 1. The $3N$ dynamic equations are

$$\begin{aligned}
\ddot{x}_i &= \frac{k_c}{m_i} \sum_{j=1}^{3} \frac{x_i - x_j}{|\vec{r}_i - \vec{r}_j|^3} q_i q_j \\
\ddot{y}_i &= \frac{k_c}{m_i} \sum_{j=1}^{3} \frac{y_i - y_j}{|\vec{r}_i - \vec{r}_j|^3} q_i q_j \\
\ddot{z}_i &= \frac{k_c}{m_i} \sum_{j=1}^{3} \frac{z_i - z_j}{|\vec{r}_i - \vec{r}_j|^3} q_i q_j
\end{aligned} \tag{3}$$

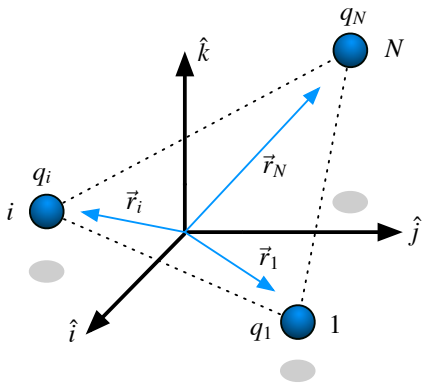

Figure 1. N bodies are shown to illustrate the body numbering, charge, and position vector notation.

where $\vec{r}_i$ is the absolute position vector from the origin of the inertial frame to the ith body with elements , $\vec{r}_i = [x_i \quad y_i \quad z_i]^T$. Finally, it is assumed that the charges on the bodies, q_i, can be set to any value, instantaneously. The control objective examined in this paper is to move the bodies from an arbitrary initial configuration into a prescribed final geometry with zero final speeds.

Although the system has $3N$ degrees of freedom, the space of possible paths is limited. More specifically, as the bodies are charged, their motion will maintain constant center of mass and angular momentum vectors. Therefore, the system cannot be made to track arbitrary paths. Another interesting restriction on the motion, from a closed loop control perspective, is that the nonlinear presentation of the control inputs, q_i, limits the ability to create arbitrary accelerations on the right side of Eq. 3.[5]

Instead of attempting to control the positions of all N bodies simultaneously, a sequential approach is used. The method is based on two observations. First, it is clear that any three bodies can be used to arbitrarily position a 4th body as long as all 4 bodies are not in a single plane. A simple approach is to set the charge on the 4th body to a constant, then adjust the charges on the other three bodies to obtain any

desired net force on the 4th body. The second observation is that any three bodies can be brought to rest by sequentially applying forces between them as long as the bodies initially started from rest.

The sequential control approach is based on the combination of these two observations. More specifically, we'll assume that in general there are 3 additional "drone" bodies whose sole purpose is to reposition the original N bodies by exploiting the first observation above. At the end of the repositioning maneuver, the three drones will be brought to rest using the second observation. A typical example is shown in Figure 2 where there are 4 bodies to be repositioned (red) and 3 drones (blue). Initially, all bodies are at rest with the four red bodies lying in the $\hat{i} - \hat{j}$ plane. At the end of the maneuver all the bodies are again motionless. The 4 red bodies have been repositioned in a specified shape. The final drone positions, however, are strictly an artifact of the operation. The sequential control strategy can now be divided into 2 phases: (1) N repositioning maneuvers, and (2) bringing the drones to rest. In the remainder of this section, control laws for both phases are developed.

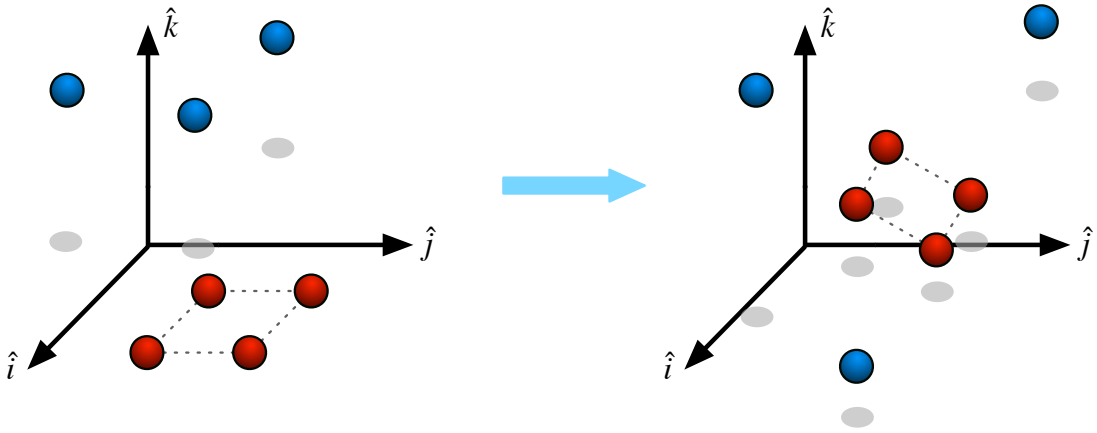

Figure 2. A typical 4-body repositioning operation showing initial and final configurations of the drones (blue) and the target bodies (red).

A. Repositioning Control

The objective of this phase of the control strategy is to use drone charging to move the $i$the body from its initial position, $\vec{r}_i$, to a desired final position, $\vec{r}_{d_i}$. The ith body is assumed to be motionless at the beginning of the operation, and it is to be motionless at the end. The drone bodies will be denoted a, b, and c, and the ith body is given a nonzero, constant charge, q_i. As long as the three drones and body i are not in the same plane, any desired net force, $\vec{f}_{d_i}$, can be imposed on body i by the drones. Ultimately, the goal is to compute the required drone charges given a desire net body i force. First, the desired net force will be written as

$$\vec{f}_{d_i} = \vec{f}_{ia} + \vec{f}_{ib} + \vec{f}_{ic} \tag{4}$$

where $\vec{f}_{ij}$ is the force imparted on body i by body j. Figure 3 illustrates the situation in addition to showing the position vector of body i, $\vec{r}_i$, and the position vector of the desired location for body i, $\vec{r}_{d_i}$. Since the direction of the Coulomb forces between the drones and body i is always line of sight, Eq. 4 can be written more explicitly as

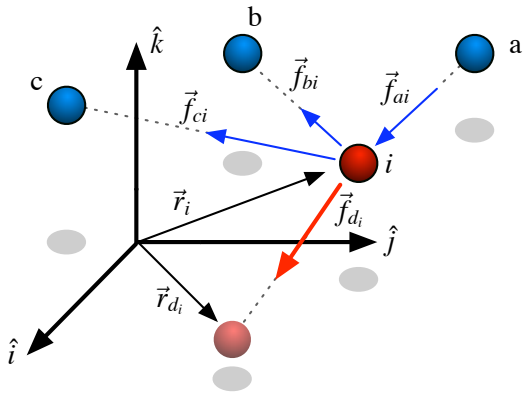

Figure 3. A typical operation of using 3 drones to reposition a single body to illustrate the drone numbering and force vector notation.

$$\vec{f}_{d_i} = f_{ia}\hat{r}_{i/a} + f_{ib}\hat{r}_{i/b} + f_{ic}\hat{r}_{i/c} \tag{5}$$

where $\hat{r}_{i/j}$ is

$$\hat{r}_{i/j} = \frac{\vec{r}_j - \vec{r}_i}{\|\vec{r}_j - \vec{r}_i\|} \tag{6}$$

The magnitudes of the drone forces can be computed as

$$\begin{Bmatrix} f_{ai} \\ f_{bi} \\ f_{ci} \end{Bmatrix} = J_i^{-1} \vec{f}_{d_i} \tag{7}$$

where

$$J_i = \begin{bmatrix} \hat{r}_{a/i} & \hat{r}_{b/i} & \hat{r}_{c/i} \end{bmatrix} \tag{8}$$

Finally, the drone charges can be computed as appropriate to the geometry of the body. For the spherical bodies considered here, Eq. 1 yields

$$q_a = \frac{f_{ai}\|\vec{r}_{a/i}\|^2}{q_i k_c} \quad q_b = \frac{f_{bi}\|\vec{r}_{b/i}\|^2}{q_i k_c} \quad q_c = \frac{f_{ci}\|\vec{r}_{c/i}\|^2}{q_i k_c} \tag{9}$$

Clearly, arbitrary net force values, $\vec{f}_{d_i}$ are only possible as long as J_i^{-1} exists. In general, body i maneuvers that are near the drone plane are impractical due to excessively large required charges.

Now that a procedure has been developed for generating arbitrary desired net forces on body i, the next step is to develop a method for moving body i from $\vec{r}_i$ to $\vec{r}_{d_i}$. Although any path that does not cross the drone plane could be used, a simple straight line approach will be employed in this development. Thus, the error in line-of-sight of distance between the current and desired position of the ith body is

$$e_i = \|\vec{r}_{d_i} - \vec{r}_i\| \tag{10}$$

and the direction of the desired control force to be exerted on body i is

$$\hat{f}_{d_i} = \frac{\vec{r}_{d_i} - \vec{r}_i}{\|\vec{r}_{d_i} - \vec{r}_i\|} \tag{11}$$

All that is left is to compute the magnitude of $\vec{f}_{d_i}$. To make the control development as general as possible, it will be assumed that any stable regulator controller is used to generate the desired force amplitude, f_{d_i} along the line-of-sight direction between the desired ith body location and its current location. For example, applying a proportional-derivative (PD) strategy would yield

$$f_{d_i} = K_{p_i} e_i + K_{d_i} \dot{e}_i \tag{12}$$

where K_{p_i} and K_{d_i} are appropriately chosen controller gains, e_i is given by Eq. 10 and $\dot{e}_i$ is

$$\dot{e}_i = -\frac{\dot{\vec{r}}_i \cdot (\vec{r}_{d_i} - \vec{r}_i)}{\|\vec{r}_{d_i} - \vec{r}_i\|^2} \tag{13}$$

It should be emphasized that any stable control strategy could be used, and that the PD example above is just for illustration.

Before proceeding on to the second phase of the control strategy, driving the drone speeds to zero, some additional discussion of the force Jacobian, J_i, is appropriate. It was mentioned above that the chief limitation of this strategy is that J_i must be nonsingular, with body i never crossing the drone plane. Although a bit premature, it may be useful to consider some "practical" methods to overcome this. Assuming that there is more than one body to reposition, one approach to avoiding singularities in J_i is to simply shift the attention of the drones from ith body to the jth whenever i gets near the drone plane. The hope is that by the time j is repositioned the drone plane will have changed sufficiently such that i is no longer near it. Although this may work in practice, it is likely not possible to prove that this approach will be robust. A second solution would be to incorporate redundancy into the drone "fleet." Since the computation of the desired net force would no longer be unique, it could be solved to ensure that there always exists 3 drones that do not lie in a plane with the ith body.

B. Drone Arrest Control

After repositioning a body the drones will likely have nonzero speeds. These should be brought to rest so they are available for additional reconfiguration operations either at the end of each repositioning operation, or after repositioning all N bodies. It should be noted that the velocity vectors of the drones, after performing a repositioning operation of body i, will all lie in the drone plane as shown in Figure 4. Additionally, the center of mass of the whole formation remains fixed, as well as the center of mass of the three drones.

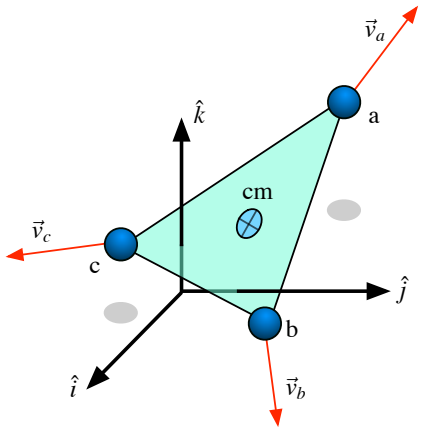

Figure 4. Illustration of the three drones, and typical velocity vectors, after repositioning body i.

The same method described in Section B will be used to halt drone motion. But instead of performing a position servo maneuver, the drones will simply be brought to rest with no regard for their final position. Arresting drone motion is performed in two steps: (1) use two bodies to halt the speed of the third, and (2) halt the motion of the remaining two moving bodies by applying a force along their line of sight motion. These two steps are covered in detail in the remainder of the section.

1. *Bringing the first drone to rest*

The general idea is to set the charge on one drone, for example a, to a nonzero constant, then use the remaining two drones, for example b and c, to drive drone c's speed to zero.

Any desired force, $\vec{f}_{d_a}$, can be imparted on drone a using Coulomb forces from drones a and b as long as $\vec{f}_{d_a}$ is in the drone plane and all three drones are not in a line. Using the same approach as in Section B, and Eq. 7, drone b and c forces can be calculated as

$$\begin{Bmatrix} f_{ba} \\ f_{ca} \\ 0 \end{Bmatrix} = J_a^{-1} \vec{f}_{d_a} \tag{14}$$

where

$$J_a = \begin{bmatrix} \hat{r}_{c/a} & \hat{r}_{b/a} & \hat{r}_{c/a} \times \hat{r}_{b/a} \end{bmatrix} \tag{15}$$

It should be noted that since all the drone velocity vectors are in the drone plane the component of $\vec{f}_{d_a}$ in the $\hat{r}_{c/a} \times \hat{r}_{b/a}$ should always be zero.

To bring drone a to rest efficiently, the direction of $\vec{f}_{d_a}$ should be opposite to the direction of $\vec{v}_a$, that is

$$\hat{f}_{d_a} = -\hat{v}_a = -\frac{\vec{v}_a}{\|\vec{v}_a\|} \tag{16}$$

The magnitude of $\vec{f}_{d_a}$ can be computed using any stable control law. One approach is to use rate feedback, which gives the desired net force vector acting on drone a as

$$\vec{f}_{d_a} = -K_{d_a} \vec{v}_a \tag{17}$$

The charges for drones b and c are readily computed as

$$q_b = \frac{f_{ba} \|\vec{r}_{b/a}\|^2}{q_a k_c} \quad q_c = \frac{f_{ca} \|\vec{r}_{c/a}\|^2}{q_a k_c} \tag{18}$$

2. *Bringing the remaining two drones to rest*

After completing the operation described in Section 1 the remaining two drones, b and c, will be moving such that their velocity vectors are coincident and along their line or sight direction, or

$$\begin{aligned} \hat{v}_b &= \pm \hat{r}_{b/c} \\ \hat{v}_c &= \pm \hat{r}_{b/c} \end{aligned} \tag{19}$$

This is illustrated in Figure 5 which also shows the line-of-sight interaction forces $\vec{f}_{bc}$ and $\vec{f}_{cb}$.

The charges on drones b and c should be controlled to arrest their relative velocity. Since the entire system started from rest, this will result in zero *absolute* velocities for both bodies. Assuming all the drone masses (m_d) are equal, the relative motion dynamic equation for this system

$$\begin{aligned} m_d\ddot{d}(t) =& f_{bc}(t) = \frac{2k_c q_b q_c}{d^2(t)} \\ d(t) =& \|\vec{r}_b(t) - \vec{r}_c(t)\| \end{aligned} \tag{20}$$

is helpful for developing the control strategy. Again, any stable control law could be employed for computing f_{bc}. A rate feedback strategy, where K_{bc} can be used to adjust the speed regulating time constant, is shown here

$$q_c = K_{bc}\frac{d^2\dot{d}}{2k_c q_b} \tag{21}$$

where q_b is a fixed, nonzero charge and

$$\dot{d} = \frac{(\vec{r}_b - \vec{r}_c)\cdot\left(\dot{\vec{r}}_b - \dot{\vec{r}}_c\right)}{\|\vec{r}_b - \vec{r}_c\|} \tag{22}$$

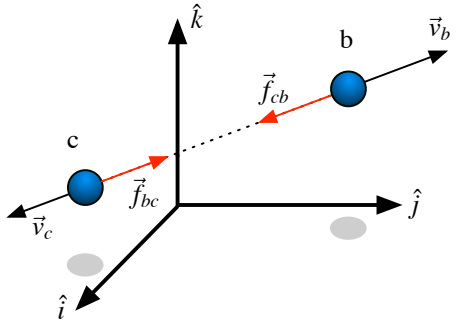

Figure 5. Illustration of the line-of-sight nature of the motion of the final two drones, and their line of sight interaction forces.

III. Three Dimensional Repositioning Example

The purpose of this example is to illustrate the application of the control laws developed in Section B. The 3 drone masses, 10 kg each, are used to reposition a single body having a mass of 1 kg. All the objects are assumed to be spherical, with a radius of 1 meter. The initial and final position vectors of all the masses are given in Table 1.

Object Type	Initial Position Vector (m)	Final Position Vector (m)
Body "1"	$[0\ 0\ 0]^T$	$[-1\ -3\ -.5]^T$
Drone "a"	$[1\ 3\ 0]^T$	Unspecified
Drone "b"	$[-3\ 2\ 0]^T$	Unspecified
Drone "c"	$[1\ 0\ 3]^T$	Unspecified

Table 1. Initial and final position vectors of body 1 and all three drones.

The total operation is simulated for 15 minutes (900 seconds) where the repositioning of body 1 occurs from $t = 0$ to $t = 400$ seconds. Next, the speed of drone "a" is brought to zero by between $t = 400$ and $t = 600$ seconds. Finally, the speeds of both drones "b" and "c" are brough to rest between $t = 600$ and $t = 800$ seconds. In all three phases of operation one of the spheres is charged to a constant level as previously described. In all cases this constant charge level was set to 1.055μC. The gains for the control laws developed in Section B were: $K_{p_1} = 0.001$, $K_{d_1} = 0.051$, $K_{d_a} = 0.25$, and $K_{bc} = 0.25$.

The simulation results are shown in Figure 6 and Figure 7. The potentials of the spherical bodies are shown in Figure 6 where the maximum voltage is approximately 30kV on drone "a". Potentials were computed from raw charges using Eq. 2. The constant charge levels are clearly evident for each phase of the control. Figure 7 shows x, y, and z components of the change in position for body "1" and all three drones. For example, the 0 position for drone "a" corresponds to $x = 1, y = 3$ and $z = 0$ meters and its final position is at approximately $x = 1.4, y = 3.9$ and $z = 0.5$ meters. It's clear that the objective of repositioning body "1" is accomplished in approximately 120 seconds.

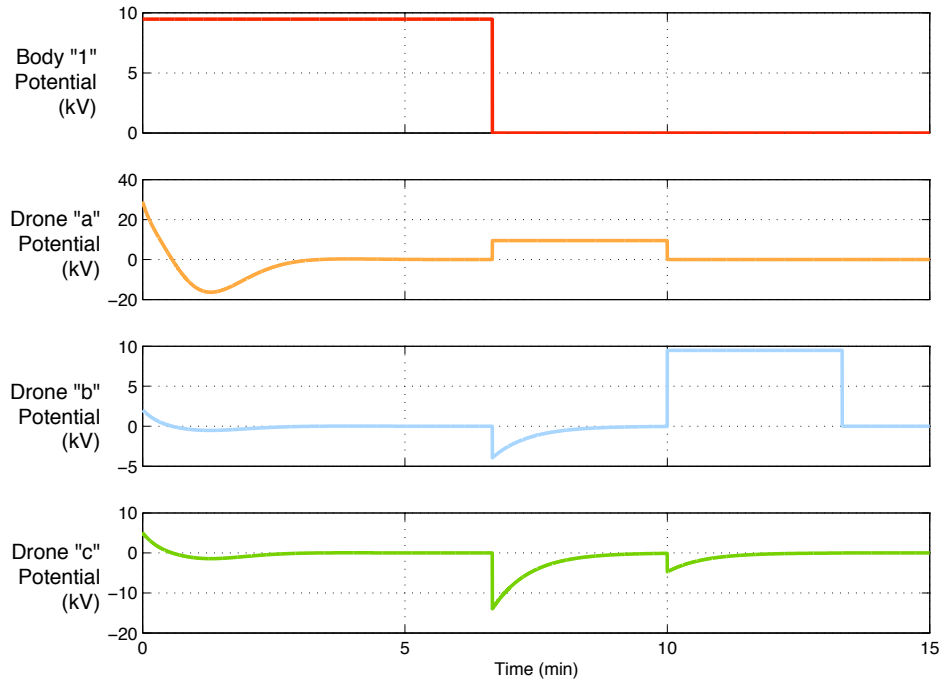

Figure 6. The potentials of body "1" and all three drones during the three phases of the example repositioning operation.

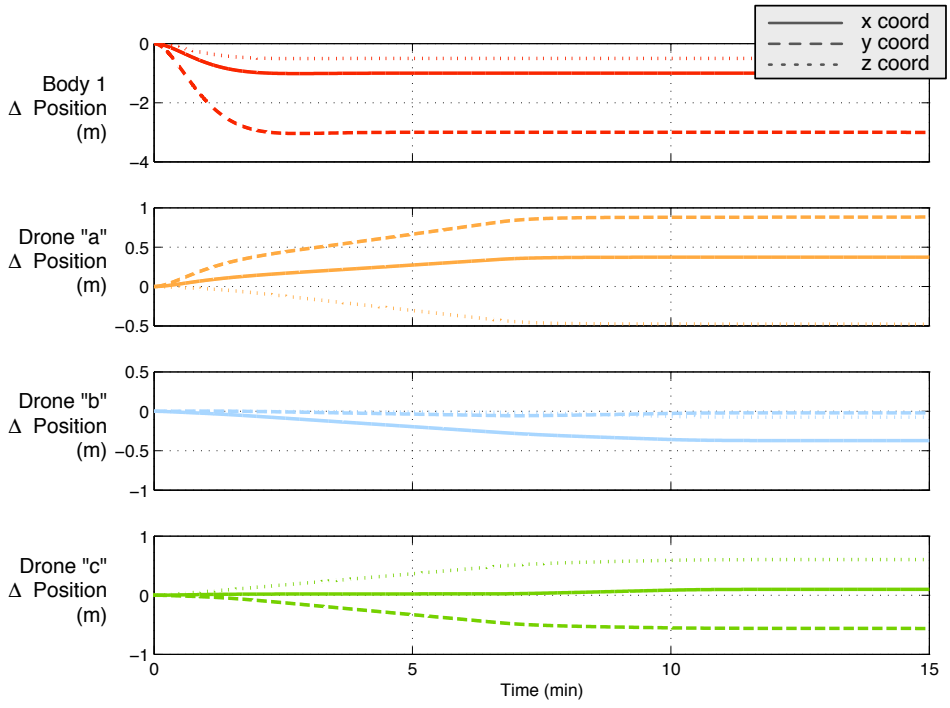

Figure 7. The x, y and z components of body "1" and all three drones during the three phases of the example repositioning operation.

IV. Conclusions

A three phase, sequential control strategy was developed for general repositioning of a charged body using 3 drones. This approach can be expanded to repositioning N bodies using the three same drones by either bringing the drones to rest after each repositioning operation, or waiting until all bodies have been relocated. Although this approach overcomes the complexity of the coupling between charged bodies when attempting simultaneous control, and removes the square nonlinearity from the problem, it does have a few practical limitations. First, when a body is being repositioned, the drones may end up far from each other, resulting in large charges to bring their speeds to zero. Second, singularities in the force Jacobians can occur if all 4 bodies are in a plane during general repositioning, or if 3 drones are in a line, during the drone arrest phase. Both of these limitations can be addressed by utilizing more drones, and an appropriate charge and trajectory management approach. For example, one set of drones could be used to move body 1. After completing the drone arrest phase, a different set of drones could be used to reposition body 2. If the trajectories of the drones are predicted then these operations may be possible such that drones can be brought back towards the main set of bodies. In short, this work has illustrated a basic approach for moving and arresting the motion of charged bodies. These fundamental methods can be applied in a variety of ways to achieve desired operations.

References

[1]King, L. B., Parker, G. G., and Chong, J.-H., "Coulomb Controlled Spacecraft Formation Flying," *AIAA Journal of Propulsion and Power*, Vol. 19, No. 3, 2003, pp. 497–505.

[2]Mullen, E. G., Gussenhoven, M. S., and Hardy, D. A., "SCATHA Survey of High-Voltage Spacecraft Charging in Sunlight," *Journal of the Geophysical Sciences*, Vol. 91, 1986, pp. 1074–1090.

[3]Garrett, H. B. and DeFrost, S. E., "An Analytical Simulation of the Geosynchronous Plasma Environment," *Planetary Space Science*, Vol. 27, 1979, pp. 1101–1109.

[4]King, L. B., Parker, G. G., Deshmukh, S., and Chong, J.-H., "A Study of Inter-Spacecraft Coulomb Forces and Implications for Formation Flying," *38th AIAA/ASME/SAE/ASEE Joint Propulsion Conference and Exhibit*, AIAA Paper No. 2002-3671, Indianapolis, IN, July 2002.

[5]Schaub, H., Parker, G. G., and King, L. B., "Challenges and Prospects of Coulomb Satellite Formation Flying," *AAS John L. Junkins Astrodynamics Symposium*, AAS Paper No. AAS03-278, College Station, TX, May 2003.